Renewable Energy 62 (2014) 129–136

Contents lists available at SciVerse ScienceDirect

Renewable Energy

journal homepage: www.elsevier.com/locate/renene

Influences of gas relative humidity on the temperature of membrane in PEMFC with interdigitated flow field

Qi-fei Jian, Guang-qing Ma*, Xiao-liang Qiu

School of Mechanical and Automobile Engineering, South China University of Technology, Guangzhou 510640, Guangdong, China

ARTICLE INFO

Article history:
Received 9 October 2011
Accepted 29 June 2013
Available online 24 July 2013

Keywords:
Interdigitated
PEM
Fuel cell
CFD modeling
Humidification
Temperature difference

ABSTRACT

A fundamental understanding of the water balance of a fuel cell during operation is crucial for improving the cell performance and durability. The humidification in the anode or cathode has an important effect on the flow characteristics and cell efficiency. Three-dimensional steady mathematical model based on the electrochemical, current distribution, fluid motion continuity equation, momentum and energy equation, boundary layer theory has been developed to simulate PEMFC with interdigitated flow field using the computational fluid dynamics (CFD). Effects on the current density and temperature differences have been simulated and analyzed respectively, when the humidification in the anode or cathode is from 0% to 100% respectively. The numerical results show that the humidification strongly influences the current density and temperature difference so as to affect the cell efficiency. Under the same operation conditions and low humidification conditions, anode humidification can better enhance the performance of the battery and improve the extent of PEM humidification.

1. Introduction

Being lightweight, ensuring environmental safety, and having high power density and immediate response to power demands, the proton exchange membrane fuel cell (PEMFC) is one of the best candidates for power sources for commercial applications [1]. The performance of proton exchange membrane fuel cell is influenced by levels of internal influential parameters such as gas flow channel design, relative humidity ratio, operation temperature and others [2]. Water balance of a fuel cell during operation is crucial for improving the cell performance and durability. The membrane electrolyte needs to be fully hydrated for meeting the function of proton conductor and it is achieved by often fully humidified anode and cathode. Along with the current density rising, the gas of lack of effective humidifying measures may be lead to dry the membrane. Opposite to that, in large current density or small airflow velocity cases, Resultant water coagulates in the hole of the cathode gas diffusion layer, forming the phenomenon of cathode flooding. Both drying and flooding are bad for battery output performance. Drying will result in greater contact resistance and ohmic resistance, so that the output voltage decreases. When severe dehydration, it will led to membrane rupture, a serious threat to the safe operation of the battery. Flooding prevents the transmission of the oxygen activation catalytic point, and gives rise to the uneven distribution of the reaction gas. While, water covers the parts of the activation catalytic surface, so that it can't be catalyzed electrochemical reaction, reducing the utilization of the catalyst, making the performance decline. And because of sometimes the water concentration, sometimes being out of gas diffusion layer, water flooding will make the battery's output voltage to be oscillated. The main purpose of water management is to prevent the drying and flooding, to maintain appropriate water content in the membrane, while water from the reaction will be discharged from the battery in a timely manner, for improving and maintaining battery performance.

In the past years, researches on PEMFC made great progress were close to commercial application. Results showed that in downstream part of the flow field, less water was held by the membrane, and electro-osmosis coefficient and ionic conduction were lower, which implied lower fuel consumption and thereby lower cell performance [3]. Kanezaki [4] and Nam [5] have found that the cross-leakage or under-rib convection flow between adjacent channels can reduce the concentration over potential and help remove liquid water effectively from the electrode structure, thus explaining an experimental result of good cell performance. Jeon et al. [6]have investigated the effect of different flow channel designs on 10 cm^2 serpentine PEMFC by comparing the distributions of over potentials, current density and membrane water content at different cell voltages at high and low inlet humidity

* Corresponding author.
E-mail addresses: tcjqf@scut.edu.cn (Q.-f. Jian), xue_657@163.com (G.-q. Ma).

0960-1481/$ – see front matter © 2013 Elsevier Ltd. All rights reserved.
http://dx.doi.org/10.1016/j.renene.2013.06.046

operating conditions, demonstrating that, for practical use, there should be a compromise between manufacturing cost and performance. At present, researches on the Humidification with interdigitated flow field on PEMFC are limited. Pil [7] and yuan [8] found that the anode humidification has more significant influences on the cell performance than the cathode humidification. The models and techniques have also been developed. Shimpalee S. et al. [9] presented a simplified technique for investigating flooding effects in an established numerical model, the conclusion shows that this technique may be improved to be more realistic when it is used in conjunction with a hydrophobic pore distribution of the gas diffuse layer. Distributions in reactant species concentration in PEMFC can lead to effects, such as flooding or drying of the membrane, Ref. [10] revealed that for stationary condition, narrower channel with wider rib spacing gives higher performance but opposite results when automotive condition is applied. The 1D model by Baschuk and Li [11], based on reactant diffusion limitations depending on an input flooding parameter, has been extended to 3D by Schwarz and Djilali [12]. Jiao and Zhou [13] found the hydrophilic surfaces result in strong wall adhesions through a three-dimensional numerical simulation of air–water flow across gas diffusion layer (GDL) with catalyst layer and serpentine channel in a PEM fuel cell, so it was difficult for water to be removed, which was not good for PEM fuel cell operation. Mather et al. [14] presented a tubular-shaped proton exchange membrane fuel cell model, and the model can provide valuable information about the transport phenomena inside the fuel cell. He et al. [15] utilized the three-dimensional two phases and non-isothermal simulation model to estimate the water effect. Li et al. [16] designed the flow channel configuration to cause an appropriate pressure drop. This can make the liquid water in the cell be evaporated and removed from, or carried out of, the cell by the gas stream in the flow channel. The behavior of liquid water in the channels has been studied by Le and Zhou [17]. They found that the removal of liquid water strongly depends on the magnitude of the flow field in the interdigitated channel PEM fuel cell. Due to the blockage of liquid water, the gas flow is unevenly distributed; the high pressure regions take place at the locations where water liquid appears.

Schematic of the flow fields in this study is interdigitated flow field, as illustrated in Fig. 1. For PEMFC with interdigitated flow field, baffles are added at the end of each flow channel to force the fuel gas transported into the gas diffusion layer by convection.

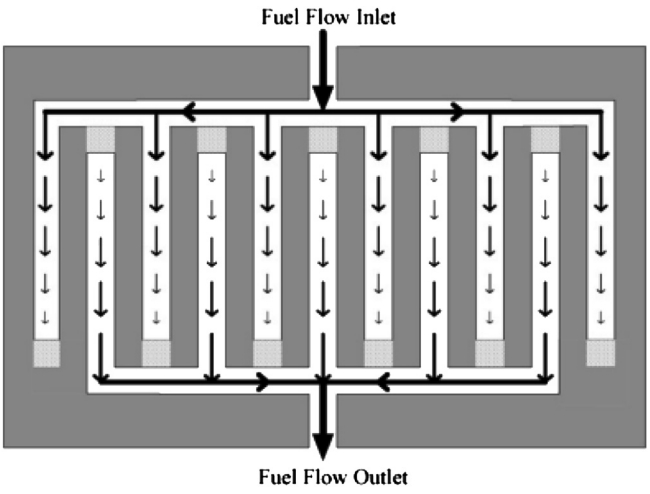

Fig. 1. Schematic of the interdigitated flow fields.

Meanwhile, the shear stress generated by the forced convection can be useful for removing redundant water, accumulated in the diffuser layer, thus the limiting current density for PEMFC with interdigitated flow field can be enhanced, and thereby PEMFC performance can be greatly improved. In short, interdigitated flow field show better performance for its advantage in mass-transport ability, but higher pressure drop for its flow through the electrode.

2. Mathematical models of PEMFC

A 3-D isothermal CFD fuel-cell model is developed to investigate the effects of different operating conditions on the performance for a high-temperature PEMFC. The assumptions on which the model is based are:

1. Both the anode and cathode side fuel are assumed to be ideal gases;
2. In flow channels, the fuel gas is laminar and incompressible;
3. The effect of gravity is ignored;
3. The effective diffusion coefficient of reactant gases in the porous media is constant;
4. The gas diffusion layer, catalyst layer and membrane are isotropic and homogeneous, characterized by effective permeability and uniform porosity;
5. The PEMFC system operates in a steady and isothermal state. With the assumptions, the governing equations are described below:

2.1. Hydraulic equations

2.1.1. Continuity equation

$$\nabla\cdot(\varepsilon\rho u) = S_{\mathrm{m}} \tag{1}$$

Where, ε is the porosity of the porous media, which is equal to unit for the gas channels, ρ the density, and u the intrinsic fluid velocity vector. S_{m} denotes the mass source term considering the electrochemical aspects of the fuel cell, thus they are zero in most of the computation domain except for the activated reaction sites as the anode and cathode catalyst layers. These terms corresponding to the consumption of hydrogen and oxygen in the anode and the cathode, and the production of water in the cathode can be determined as following:

$$S_{\mathrm{m}} = \sum_{k} S_k \tag{2}$$

Where S_{k} stands for the source/sink term of the k'th species induced by the electrochemical reaction occurred in the active catalyst layers.

2.1.2. Momentum equation

$$\nabla\cdot(\varepsilon\rho v u) = -\varepsilon\nabla p + \left(\varepsilon v_{\mathrm{eff}}\nabla u\right) + S_{\mathrm{U}} \tag{3}$$

Where

$$S_{\mathrm{U}} = -\frac{\mu_{\mathrm{eff}}\varepsilon^2 U}{k} \tag{4}$$

Where p is pressure, v_{eff} is effective viscosity, S_{U} is source term vector of momentum equation, k is permeability of porous electrode.

2.1.3. Energy equation

$$\nabla\cdot\left(\lambda_{\text{eff}}\nabla T\right) = \nabla\cdot\left(\varepsilon\rho C_{\text{p}}uT\right) + S_{\text{h}} \tag{5}$$

where,

$$S_{\text{h}} = I^2R_{\text{ohm}} + h_{\text{reaction}} + \eta j_{\text{a,c}} + h_{\text{phase}} \tag{6}$$

$$h_{\text{phase}} = r_{\text{w}}h \tag{7}$$

$$r_{\text{w}} = c_{\text{r}}\max\left[(1-\chi)\frac{p_{\text{wv}}-p_{\text{sat}}}{R_{\text{g}}T}M_{\text{W,H}_2\text{O}} - s\rho_1\right. \tag{8}$$

Where λ_{eff} is effective thermal conductivity, Cp is the isobaric heat; S_{h} is source terms of energy. I is the local current density. h_{reaction} is heat of formation of water. h_{phase} is heat of condensation. j_{a} is exchange current density of anode and j_{c} is exchange current density of cathode. η is the local over potential. r_{w} is the condensation. χ is the volume fraction of liquid water.

2.1.4. Components equation

In the presence of a velocity field, various chemical flow fields are component of the convective flow and diffusion flow. For the component of chemical reactions(H_2, O_2, H_2O), general transfer equation can be expressed

$$\nabla\cdot(\varepsilon\rho uY_{\text{i}}) = \nabla\cdot\left(\rho D_{\text{i}\cdot\text{eff}}\nabla Y_{\text{i}}\right) + S_{\text{i}} \tag{9}$$

Where Y_{i} is the mass fraction. $D_{\text{i}\cdot\text{eff}}$ is the effective diffusion coefficient. S_{i} is the component Source. I in the anode means component code of H_2 and i in the cathode means component code of O_2 and H_2O.their component Source means:

$$S_{\text{H}_2} = -\frac{1}{2\text{FC}_{\text{H}_2}}j_{\text{a}} \tag{10}$$

$$S_{\text{O}_2} = \frac{1}{4\text{FC}_{\text{O}_2}}j_{\text{c}} \tag{11}$$

$$S_{\text{H}_2\text{O}} = -\frac{1}{2\text{FC}_{\text{H}_2\text{O}}}j_{\text{c}} \tag{12}$$

2.2. Electrochemical models

The electrical potentials of the membrane phase φ_{m} and carbon phase φ_{a}, φ_{c} are introduced following the concept of mean parameters. The two types of potentials manage the motion of protons and that of electrons, respectively. Taking local electroneutrality into account, the electronic current and ionic current produced or consumed in the catalyst layers leading to a voltage drop via Ohm's law according to:

$$\nabla(\sigma_{\text{s}}\nabla\varphi_{\text{s}}) + j_{\text{s}} = 0 \tag{13}$$

$$\nabla(\sigma_{\text{m}}\nabla\varphi_{\text{m}}) + j_{\text{m}} = 0 \tag{14}$$

For the anode side:

$$j_{\text{s}} = -j_{\text{a}} < 0, \quad j_{\text{m}} = +j_{\text{a}} > 0 \tag{15}$$

For the cathode side:

$$j_{\text{s}} = +j_{\text{c}} > 0, \quad j_{\text{m}} = -j_{\text{c}} < 0 \tag{16}$$

After obtaining the phase potentials, the current density in the external circuit I can be calculated by the following expression:

$$I = \frac{1}{H}\times\frac{1}{L}\times\int_0^H\int_0^L\left(\sigma_m\frac{\partial\varphi_m}{\partial x}\Big|_{x=x_3}\right)\text{dydz} \tag{17}$$

Where H is the height of the catalyst layer, L is the length. As $\varphi_a|_{x=x_0}$ is taken to be zero, then $\varphi_c|_{x=x5} - \varphi_a|_{x=x0} = \varphi_c|_{x=x5}$ gives total voltage of the whole fuel cell [18].

The over-potential η is computed as:

$$\eta = \phi_{\text{c}} - \phi_{\text{m}} - V_{\text{ref}} \tag{18}$$

For the anode side:

$$\eta_{\text{a}} = \phi_{\text{c}} - \phi_{\text{m}} \tag{19}$$

For the cathode side:

$$\eta_{\text{a}} = \phi_{\text{c}} - \phi_{\text{m}} - V_{\text{oc}} \tag{20}$$

The j_{a} and j_{c} terms are the exchange current density at the anode side and the cathode side, as calculated from Bulter–Volmer expression:

$$j_{\text{a}} = j_{\text{a}}^{\text{ref}}\left(\frac{C_{\text{H}_2}}{C_{\text{H}_2}^{\text{ref}}}\right)^{\gamma_a}\left(e^{\frac{\alpha_{\text{a}}F}{RT}\eta_{\text{a}}} - e^{-\frac{\alpha_{\text{a}}F}{RT}\eta_{\text{a}}}\right) \tag{21}$$

$$j_{\text{c}} = j_{\text{c}}^{\text{ref}}\left(\frac{C_{\text{O}_2}}{C_{\text{O}_2}^{\text{ref}}}\right)^{\gamma_c}\left(e^{\frac{\alpha_{\text{c}}F}{RT}\eta_{\text{c}}} - e^{-\frac{\alpha_{\text{c}}F}{RT}\eta_{\text{c}}}\right) \tag{22}$$

2.3. Boundary conditions

The boundary conditions in this work are expressed as general expressions [19]. In this work, on the both sides, relative humilities are of 0%, 50% and 100%. And the operating pressure is 1 atm while the operating and inlet fuel temperature are 353.15 K. The operational cell voltage is 0.5 V. Boundary conditions for the model simulation described as below:

At the anode side fuel gas inlet, the boundary type is mass-flow-inlet:

$$\mu = 0, \nu = 0, w = w_{\text{in}}^{\text{a}}, C_{\text{H}_2} = C_{\text{H}_2,\text{in}}^{\text{a}}$$

$$C_{\text{H}_2\text{O}} = C_{\text{H}_2\text{O,in}}^{\text{a}} \tag{23}$$

At the cathode side fuel gas inlet, the boundary type is mass-flow-inlet :

$$\mu = 0, \nu = 0, w = w_{\text{in}}^{\text{c}}, C_{\text{H}_2} = C_{\text{H}_2,\text{in}}^{\text{c}}$$

$$C_{\text{H}_2\text{O}} = C_{\text{H}_2\text{O,in}}^{\text{c}}, C_{\text{N}_2} = C_{\text{N}_2,\text{in}}^{\text{c}} \tag{24}$$

At the fuels gas channels outlet, the boundary type is pressure-outlet:

$$\mu = \frac{\partial C_w}{\partial z} = \nu = \frac{\partial C_k}{\partial z} = 0 \tag{25}$$

At the interfaces between the fuel gas channels and plate collectors, both on the anode side and cathode side,

$$\mu = \nu = w = \frac{\partial C_k}{\partial x} = 0 \tag{26}$$

At the interfaces between the gas channels and the gas diffuser layer, both on the anode side and cathode side,

$$\varepsilon_{\text{eff}},\text{GDL}\frac{\partial\mu}{\partial y}\Big|_{y=\text{YGDL}} = \varepsilon_{\text{eff}},\text{GC}\frac{\partial\mu}{\partial y}\Big|_{y=\text{YGC}},$$

$$\varepsilon_{\text{eff}},\text{GDL}\frac{\partial v}{\partial y}\Big|_{y=\text{YGDL}} = \varepsilon_{\text{eff}},\text{GC}\frac{\partial v}{\partial y}\Big|_{y=\text{YGC}},$$

$$\varepsilon_{\text{eff}},\text{GDL}\frac{\partial w}{\partial y}\Big|_{y=\text{YGDL}} = \varepsilon_{\text{eff}},\text{GC}\frac{\partial w}{\partial y}\Big|_{y=\text{YGC}},$$

$$\mu_y = Y_{\text{GDL}} = \mu_y = Y_{\text{GC}}, v_y = Y_{\text{GDL}} = v_y = Y_{\text{GC}}, w_y = Y_{\text{GDL}} = w_y = Y_{\text{GC}},$$

$$\varepsilon_{\text{eff}},\text{GDL}\frac{\partial Ck}{\partial y}\Big|_{y=\text{YGDL}} = \varepsilon_{\text{eff}},\text{GC}\frac{\partial Ck}{\partial y}\Big|_{y=\text{YGC}},$$

$$C_{k,y} = Y_{\text{GDL}} = C_{k,y} = Y_{\text{GC}} \tag{27}$$

At the interfaces between gas diffuser layer and the catalyst layer, both on the anode side and cathode side,

$$\varepsilon_{\text{eff}},\text{GDL}\frac{\partial\mu}{\partial y}\Big|_{y=\text{YGDL}} = \varepsilon_{\text{eff}},\text{CL}\frac{\partial\mu}{\partial y}\Big|_{y=\text{YCL}},$$

$$\varepsilon_{\text{eff}},\text{GDL}\frac{\partial v}{\partial y}\Big|_{y=\text{YGDL}} = \varepsilon_{\text{eff}},\text{CL}\frac{\partial v}{\partial y}\Big|_{y=\text{YCL}},$$

$$\varepsilon_{\text{eff}},\text{GDL}\frac{\partial w}{\partial y}\Big|_{y=\text{YGDL}} = \varepsilon_{\text{eff}},\text{CL}\frac{\partial w}{\partial y}\Big|_{y=\text{YCL}},$$

$$\mu_y = Y_{\text{GDL}} = \mu_y = Y_{\text{CL}}, v_y = Y_{\text{GDL}} = v_y = Y_{\text{CL}}, w_y = Y_{\text{GDL}} = w_y = Y_{\text{CL}},$$

$$\varepsilon_{\text{eff}},\text{GDL}\frac{\partial Ck}{\partial y}\Big|_{y=\text{YGDL}} = \varepsilon_{\text{eff}},\text{CL}\frac{\partial Ck}{\partial y}\Big|_{y=\text{YCL}},$$

$$C_{k,y} = Y_{\text{GDL}} = C_{k,y} = Y_{\text{CL}} \tag{28}$$

At the interfaces between the catalyst layer and the membrane, both on the anode side and cathode side,

$$\varepsilon_{\text{eff}},\text{CL}\frac{\partial\mu}{\partial y}\Big|_{y=\text{YCL}} = 0,\ \varepsilon_{\text{eff}},\text{CL}\frac{\partial v}{\partial y}\Big|_{y=\text{YCL}} = 0,\ \varepsilon_{\text{eff}},\text{CL}\frac{\partial w}{\partial y}\Big|_{y=\text{YCL}} = 0,$$

$$\mu_y = Y_{\text{CL}} = v_y = Y_{\text{CL}} = w_y = Y_{\text{CL}} = 0,$$

$$\varepsilon_{\text{eff}},\text{CL}\frac{\partial Ck}{\partial y}\Big|_{y=\text{YCL}} = 0 \tag{29}$$

In PEMFC, water in the proton exchange membrane is transported cause by proton transport and the electro-osmotic phenomenon. Therefore, for the water transport, the velocity, the flux and the shear stress at the interfaces of catalyst layer and the proton exchange membrane must be considered to be continuously distributed. Additionally, the saturation concentration of liquid water, C_S, and the concentration flux must be continuous, which are applied in the following boundary conditions.

$$\varepsilon\text{eff},\text{mem}\frac{\partial\mu}{\partial y}\Big|_{y=Y_{\text{mem}}} = \varepsilon_{\text{eff}},\text{CL}\frac{\partial\mu}{\partial y}\Big|_{y=\text{YCL}},$$

$$\varepsilon_{\text{eff}},\text{mem}\frac{\partial v}{\partial y}\Big|_{y=Y_{\text{mem}}} = \varepsilon_{\text{eff}},\text{CL}\frac{\partial v}{\partial y}\Big|_{y=\text{YCL}},$$

$$\varepsilon_{\text{eff}},\text{mem}\frac{\partial w}{\partial y}\Big|_{y=Y_{\text{mem}}} = \varepsilon_{\text{eff}},\text{CL}\frac{\partial w}{\partial y}\Big|_{y=\text{YCL}},$$

$$\mu_y = Y_{\text{mem}} = \mu_y = Y_{\text{CL}}, v_y = Y_{\text{mem}} = v_y = Y_{\text{CL}}, w_y = Y_{\text{mem}} = w_y = Y_{\text{CL}},$$

$$\varepsilon_{\text{eff}},\text{mem}\frac{\partial CS}{\partial y}\Big|_{y=Y_{\text{mem}}} = \varepsilon_{\text{eff}},\text{CL}\frac{\partial CS}{\partial y}\Big|_{y=\text{YCL}},$$

$$C_{S,y} = Y_{\text{mem}} = C_{S,y} = Y_{\text{CL}} \tag{30}$$

The boundary condition of phase potential at the interface between the catalyst layer and the membrane is,

$$\Phi_{\text{CL}} = \Phi_{\text{mem}}, \varepsilon_{\text{eff}},\text{CL}\frac{\partial\Phi_{\text{CL}}}{\partial y} = \frac{\partial\Phi_{\text{mem}}}{\partial y} \tag{31}$$

3. Geometric model and simulation

The three-dimensional PEMFC, with interdigitated flow field, systems employed in this study is illustrated schematically in Fig. 2. The model consists of anode bipolar plate, anode flow channel, anode gas diffusion layer, anode catalyst layer, proton exchange membrane, cathode catalyst layer, cathode gas diffusion layer, cathode flow channel, cathode bipolar plate and cathode flow channel. The simulation domains consist of 583000 hexahedral cells 1813730 quadrilateral faces and 645426 nodes. The minimum hexahedral volume is 1.9999987e-13m^3, and the maximum hexahedral volume is 5.000048e-12m^3. Table 1 presents the geometric and the number of discretization:

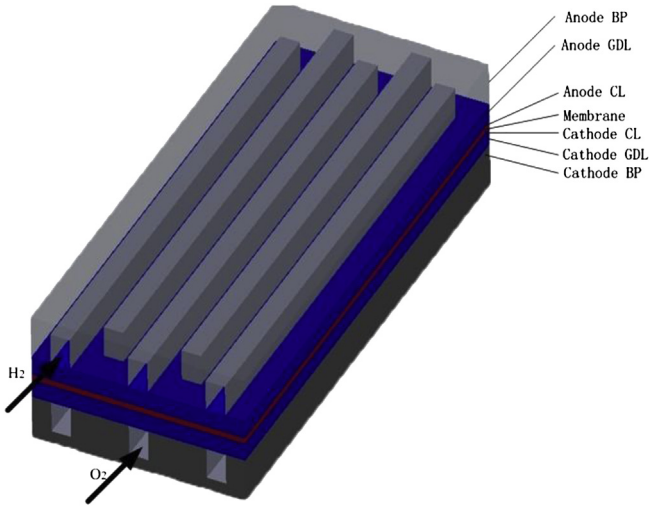

Fig. 2. 3D structure of PEMFC.

Table 1
Geometric and Discretization of the PEMFC.

	Length (mm)/discrete number	Width (mm)/discrete number	Depth (m)/discrete number
PEM	50/100	11/110	0.05/5
Catalyst layer	50/100	11/110	0.005/5
Gas diffusion layer	50/100	11/110	0.2/5
Gas flow channel	49/98	1/10	1/10
Current collector	50/100	11/110	1.4/14

The study uses the CFD software FLUTENT. A control volume technique was used to solve the model equation. Convective terms and diffusion terms are respectively discredited in space with the second-order upwind scheme and central-difference scheme. The solution is considered to be convergent when the relative residual between two consecutive iterative is less than 1.0e-6. The computations were preformed on a computer with a 3.2 GHz double processor and 32.00 GB of memory. A single solution requires about 5000 iterations. Table 2 presents physical parameters and operational parameters of the PEMFC adopted in the simulation.

4. Results and discussion

4.1. Effects of anode humidification on temperature difference

As shown in Fig. 3, when cathode humidification is respectively 0%, 50% and 100%, the range of anode relative humidity is from 0% to 100%, temperature difference on membrane of PEMFC with interdigitated flow field shows different changes. In the case of relative humidity of reactant air is 0% or 50% on cathode side, temperature difference on membrane of PEMFC increases as the anode side relative humidity increases. And in relative humidity of reactant air is 100% on cathode side situation, temperature difference on membrane increases as the anode side relative humidity increases firstly and then shows a sharp decline while relative humidity is from 75% to 100% on anode side. This is because increase of humidity on anode side improves the proton conductivity of the electrolyte and enhances the electrochemical reaction rate, meanwhile more heat generates and PEM temperature difference increases; However, when the reactant gas is extremely humidified, the concentration polarization will be worsened and reduce the battery's performance, further, water takes away more heat of PEM when water is discharged, and PEM temperature difference declines.

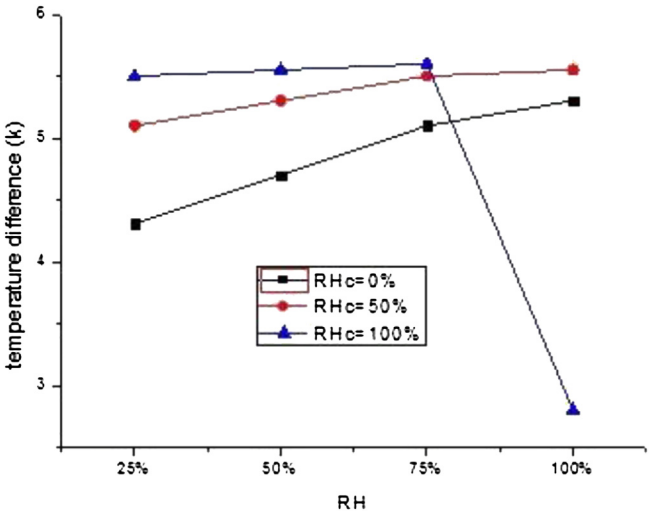

Fig. 3. Effects of anode humidification on temperature difference of PEMFC.

As presented in Fig. 4. When relative humidity on cathode side is 50%, the effects of anode humidification on the temperature of the membrane center under the inlet channels show different changes. The greater relative humidity is, the more even temperature curve is. With the humidity level of change, the temperature change of the membrane center under the inlet channels is not obvious.

Fig. 5 shows the temperature distribution curve of the membrane center under the outlet channels on the anode different humidification when cathode humidification is 50%. According to

Table 2
Operational and Physical parameters of the PEMFC.

Properties	Value
Operating pressure (atm)	1
Outlet backpressure (atm)	0
Temperature (K)	353
Contact resistance (ohm m^2)	2e-06
Electrical conductivity of current collector [1/(ohm m)]	8.3e+04
Thermal conductivity of current collector [W/(m K)]	85.5
C_p of current collector [J/(kg K)]	691
Density of current collector (kg/m^3)	1880
Electrical conductivity of gas diffusion layer [1/(ohm m)]	1000
Open circuit voltage (V)	1.05
Anode exchange current density (A/m^3)	2e+09
Cathode exchange current density (A/m^3)	1e+05
Anode concentration exponent	0.5
Cathode concentration exponent	1
Anode exchange coefficient	1
Cathode exchange coefficient	1.25
Porosity of gas diffusion layer	0.5
Thermal conductivity of gas diffusion layer [W/(m K)]	1.6
C_p of gas diffusion layer [J/(kg K)]	710
Density of gas diffusion layer (kg/m^3)	440
Thermal conductivity of membrane [W/(m K)]	2
C_p of membrane [J/(kg K)]	2000
Protonic conduction coefficient of membrane	1
Protonic conduction exponent of membrane	1
Density of membrane (kg/m^3)	1980
Equivalent weight coefficient of membrane (kg/kmol)	1100
Surface-to-volume ratio of catalyst layer (1/m)	2e+05
Electrical conductivity of catalyst layer [1/(ohm m)]	1000
Porosity of catalyst layer	0.475
Thermal conductivity of catalyst layer [W/(m K)]	8
C_p of catalyst layer [J/(kg K)]	710
Density of catalyst layer (kg/m^3)	2010

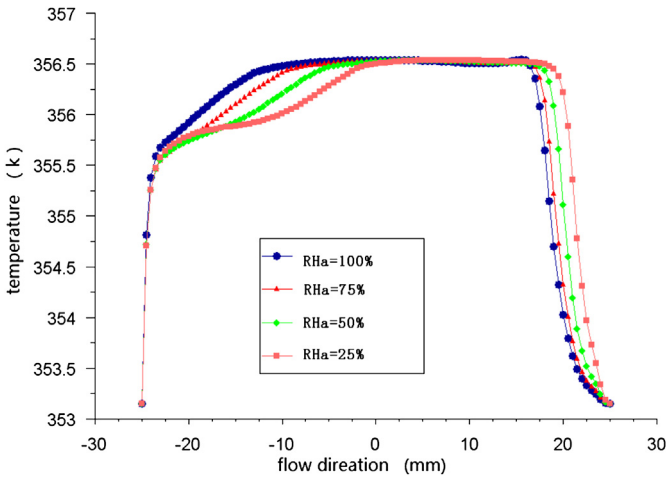

Fig. 4. Effects of anode humidification on temperature distribution of the membrane center under the inlet channels.

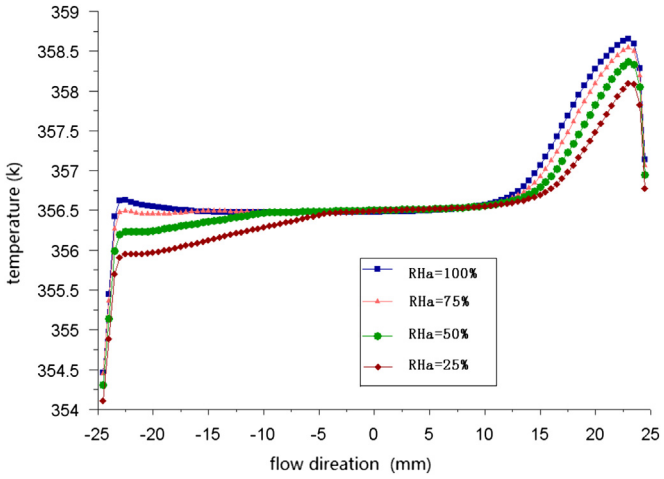

Fig. 5. Effects of anode humidification on temperature distribution of the membrane center under the outlet channels.

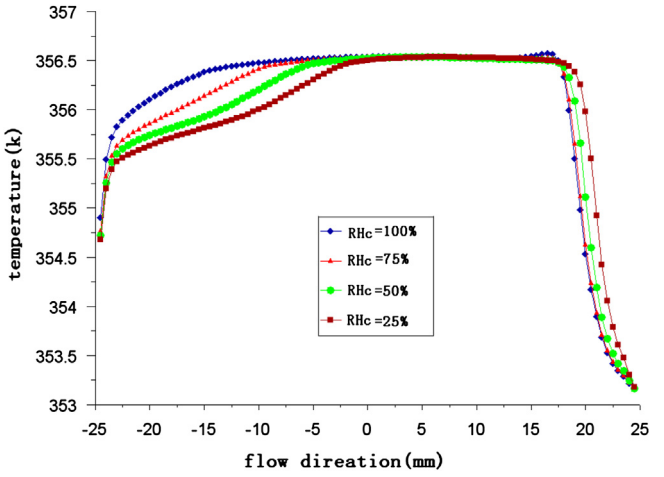

Fig. 7. Effects of cathode humidification on temperature distribution of the membrane center under the inlet channels.

Fig. 5, we can know temperature of the membrane center under the outlet channels become more and more stable with the increase degree of humidification. In the case of anode humidification is 100%, the curve is the most even and the temperature is the highest. This is because increasing humidity degree improve the proton conductivity of the electrolyte, enhance the electrochemical reaction rate and make the temperature reach the highest in advance, so electrochemical and temperature is stable [9].

4.2. Effects of cathode humidification on PEM temperature difference

In Fig. 6 we can find that: when anode humidification is respectively 0% 50% and 100%, the effects of cathode humidification on PEM temperature difference of PEMFC with interdigitated flow field show different changes. In the case of relative humidity of anode is 0% or 50%, PEM temperature difference of PEMFC increases as the cathode side relative humidity increase. And when relative humidity of anode is 100%, PEM temperature difference of PEMFC increases as the cathode side relative humidity increases firstly and then decreases, and shows a sharp decline while relative humidity is from 75% to 100% on cathode side. This is because increase of humidity on cathode side improves the proton conductivity of the electrolyte and enhances the electrochemical reaction rate, meanwhile more heat generates and PEM temperature difference increases. However, in the case of the reactant gas is extremely humidified, the concentration polarization will be worsened and reduce the battery's performance, further, water takes away more heat of PEM when water is discharged, and PEM temperature difference declines.

As shown in Fig. 7. When relative humidity on anode side is 50%, the effects of cathode humidification on the temperature of the membrane center under the inlet channels show different change. Fig. 7 shows the greater relative humidity is, the more even temperature curve is. With the humidity degree of change, the temperature change of the membrane center under the inlet channels is not obvious.

Fig. 8 shows the temperature distribution curve of the membrane center under the outlet channels on the cathode different humidification when anode humidification is 50%. According to Fig. 8, we can know temperature of the membrane center under the outlet channels become more and more stable with the increase

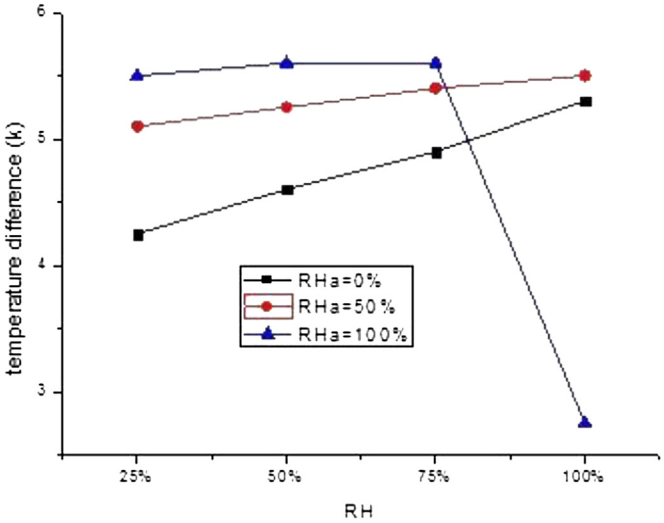

Fig. 6. Effects of cathode humidification on temperature difference distribution of the membrane.

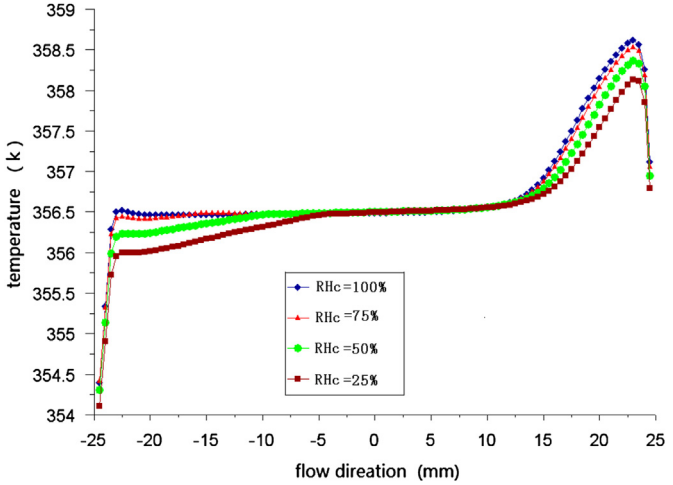

Fig. 8. Effects of cathode humidification on temperature distribution of the membrane center under the outlet channels.

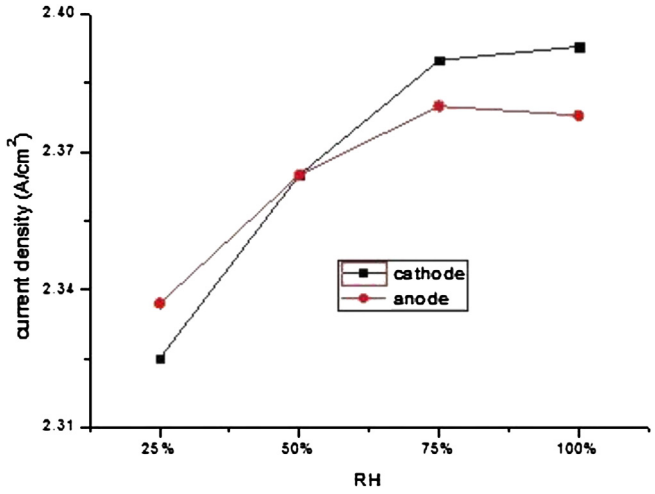

Fig. 9. Effects of anode and cathode humidification on current density of PEMFC with interdigitated flow field.

degree of humidification. In the case of cathode humidification is 100%, the curve is the most even and the temperature is the highest. Because increasing humidity degree improve the proton conductivity of the electrolyte, enhance the electrochemical reaction rate and make the temperature reach the highest in advance, so electrochemical and temperature is stable. From the three pictures, we can know the conclusion which is cathode humidification is same to the anode humidification.

4.3. Comparison of effects anode and cathode humidification on PEM temperature difference and current density

Fig. 9 is the current density change curve on the different anode and cathode humidification when anode and cathode humidification is respectively 50%. Fig. 9 shows two curves have upward trend and anode humidification can better enhance the performance of cell in the case of low humidification. The reason is that PEM transfers the protons by the generated water when humidification is inadequate. The number of protons passed is greater with the increase of humidifying degree at the same time to increase battery performance.

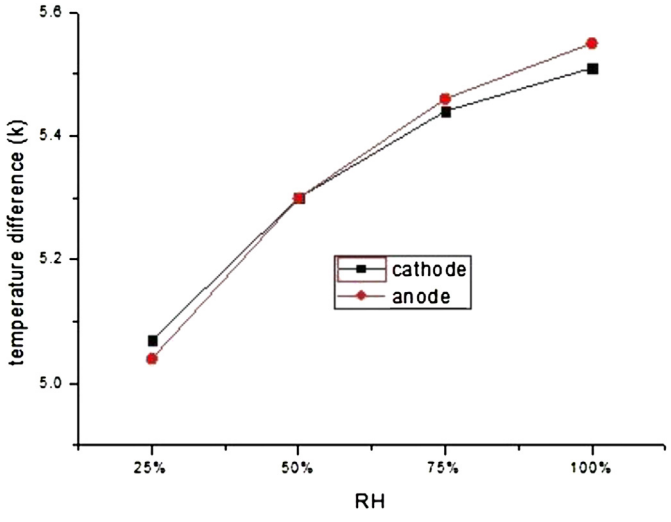

Fig. 10. Effects of anode and cathode humidification on PEM temperature difference of PEMFC with interdigitated flow field.

The temperature difference curve of the membrane on the different humidification in the cathode and anode is presented in Fig. 10 when anode and cathode humidification is respectively 50%. From the picture, we can find two curves show an increasing trend and anode humidification can better improve the humidity degree of PEM in the case of low humidity. This is because the generated water which is mainly generated in the cathode can help wetting the membrane of the cathode side.

5. Conclusions

The steady-state, three-dimensional mathematical model has been employed to investigate the PEMFC with the interdigitated flow field. The model is based on the commercial CFD software Fluent. The current density and temperature difference in the different humidification of anode and cathode on the PEMFC are detailed analyzed. Results show that in the case of the given humidification on one electrode side and changing humidity on the other electrode side, PEM temperature difference shows the same variation as the changing humidification. When anode or cathode humidification is 0% or 50%, PEM temperature difference increases as the increase degree of the other electrode humidification. When anode or cathode humidification is 100%, PEM temperature difference increases as the other electrode humidification increases firstly and shows a sharp decline while relative humidity is from 75% to 100%. Under the same operation conditions and low humidification conditions, anode humidification can better enhance the performance of the battery and improve the extent of PEM humidity.

Acknowledgments

This research was supported by the National Nature Science Foundation of China (No. 50930005), the PhD Programs Foundation of Ministry of Education of China (20100172110001) and the Guangdong Province Science and Technology Program (No. 2012B091100330, 2011A090200075).

References

[1] Ferng YM, Su A. A three-dimensional full-cell CFD model used to investigate the effects of different flow channel designs on PEMFC performance. J Hydrogen Energy 2007;32:4466–76.
[2] Cheng SJ, Miao JM, Wu SJ. Investigating the effects of operational factors on PEMFC performance based on CFD simulations using a three-level full-factorial design. J Renewable Energy 2012;39:250–60.
[3] Yan WM, Chen CY, Mei SC, Soong CY, Chen F. Effects of operating conditions on cell performance of PEM fuel ells with conventional or interdigitated flow field. J Power Sources 2006;162:1157–64.
[4] Kanezaki T, Li X, Baschuk JJ. Cross-leakage flow between adjacent flow channels in PEM fuel cells. J Power Source 2006;162:415–25.
[5] Nam JH, Lee KJ, Sohn S, Kim CH. Multi-pass serpentine flow-fields to enhance under-rib convection in polymer electrolyte membrane fuel cells: design and geometrical characterization. J Power Source 2006;188:14–23.
[6] Jeon DH, Greenway S, Shimpalee S, Van Zee JW. The effect of serpentine flow-field designs on PEM fuel cell performance. J Hydrogen Energy 2008;33:1052–66.
[7] Pil HL, Bong IP, Sang SH. Three dimensional computational study on proton exchange membrane fuel cell by operation conditions. J Thermal Sci Technol 2010;5(1):178–88.
[8] Yuan W, Tang Y, Pan Minqiang, Li ZT, Tang Biao. Model prediction of operating parameters on proton exchange membrane fuel cell performance. J Renewable Energy 2010;35:656–66.
[9] Shimpalee S, Beuscher U, Van Zee JW. Analysis of GDL flooding effects on PEMFC performance. Electrochim Acta 2007;52:6748–54.
[10] Shimpalee S, Van Zee JW. Numerical studies on rib & channel dimension of flow-field performance. Int J Hydrogen Energy 2007;32:842–56.
[11] Baschuk JJ, Li X. Modeling of polymer electrolyte membrane fuel cells with variable degrees of water flooding. J Power Sources 2000;86:181–96.
[12] Mather AR, AL-Baghdadi Sadiq. Three-dimensional computational fluid dynamics model of a tubular-shaped PEM fuel cell. J Renewable Energy 2008;33:1334–45.
[13] Schwarz DH, Djilali N. 3D modeling of catalyst layers in PEM fuel cells: effects of transport limitations. J Electrochem Soc 2007;154:B1167–78.

[14] He G, Yamazaki Y, Abudula A. A droplet size dependent multiphase mixture model for two phase flow in PEMFCs. J Power Sources 2009;194:190–8.
[15] Li X, Sabir I, Park J. A flow channel design procedure for PEM fuel cells with effective water removal. J Power Sources 2007;163:933–42.
[16] Le AD, Zhou B. A generalized numerical model for liquid water in a proton exchange membrane fuel cell with interdigitated design. J Power Sources 2009;193:665–83.
[17] Kui J, Li XG. Water transport in polymer electrolyte membrane fuel cells[J]. Prog Energy Combust Sci 2011;37:221–91.
[18] Hu GL, Fan JR, Chen S, Liu YJ, Cen KF. Three-dimensional numerical analysis of proton exchange membrane fuel cells with conventional and interdigitated flow fields. J Power Sources 2004;136:1–9.
[19] Lee CI, Chu HS. Effects of cathode humidification on the gas-liquid interface location in a PEM fuel cell. J Power Sources 2006;161:949–56.

Glossary

C: molar concentration, mol cm^{-3}
C_P: isobaric heat, J/(kg K)
D: diffusion coefficient, $cm^2\ s^{-1}$
F: Faraday constant = 96,487 C/mol
H: cell height, cm
I: mean current density, A cm^{-2}
j: transfer current density, A cm^{-3}
k: permeability of porous electrode, cm^2
L: catalyst layer width, cm
p: pressure, atm
T: cell temperature, K
R: Resistance, ohm
R_g: gas constant, J/(mol K)
S: stoichiometric coefficient
u: velocity vector, cm s^{-1}
Y_i: mass fraction
h: Generated heat, W/m^2
r_w: condensation rate

Greek letters
χ: volume fraction of liquid water
λ: thermal conductivity, W/(m K)α transfer coefficient
υ: fluid viscosity, kg $cm^{-1}\ s^{-1}$
μ,ν,ω: velocity in the *X,Y,Z* direction, cm s^{-1}
η: local over potential, V
ε: porosity of the porous media
ρ: density of the fluid, mol cm^{-3}
σ: conductivity, $\Omega^{-1}\ cm^{-1}$
φ: potential, V

Subscripts
i: component
eff: effective value
a: anode
c: cathode
f: membrane species (the fixed charge site species)
m: membrane
ref: reference
w: water